

# Applications of the mean-field lattice Boltzmann method for solid–fluid interfaces to study interfacial phenomena

Junfeng Zhang, Daniel Y. Kwok\*

*Nanoscale Technology and Engineering Laboratory, Department of Mechanical Engineering, University of Alberta, Edmonton, Alberta T6G 2G8, Canada*

---

## Abstract

We summarize our recent studies on solid–fluid interfaces using a mean-field free-energy lattice Boltzmann scheme. Results show that contact angles on smooth and heterogeneous surfaces are determined by the surface properties near the contact point and not those between the solid–liquid interface. This finding implies the invalidity of Cassie’s equation in macroscopic contact angle measurements. Apparent liquid slip was also observed over a no-slip solid fluid interface due to specific solid–fluid interactions: the weaker the interactions, the larger the contact angle and slip magnitude. These simulations have demonstrated the potential of this mean-field free-energy lattice Boltzmann model in fluid interfacial studies.

*Keywords:* Lattice Boltzmann method; Solid–fluid interactions; Contact angle; Cassie’s equation; Heterogeneous surface; Solid–fluid interfacial slip

---

## 1. Introduction

The lattice Boltzmann method (LBM) has experienced rapid development in simulating fluid behaviors during the past decade. As an extension of the lattice gas automata (LGA), the LBM describes macroscopic complex flows by dealing with the underlying micro-world. Moreover, as a mesoscopic approach that is between microscopic molecular dynamics (MD) and conventional macroscopic fluid dynamics, the LBM can be useful when microscopic statistics and macroscopic description of flow are both important. Recently, we have proposed a free-energy approach to the LBM for solid–fluid interfaces by means of a mean-field representation [1], as solid–fluid interactions are expected to play a vital role in interfacial phenomena. In this model, the solid–fluid interactions represented are physically more realistic when compared with other similar models. In this paper, we summarize two interfacial studies as performed by our mean-field LBM scheme: (1) liquid wettability on heterogeneous surfaces and (2) apparent solid–liquid interfacial slip with a no-slip boundary condition (BC).

## 2. Wettability on heterogeneous surfaces

Cassie was the first to propose a model of contact angle on a heterogeneous surface [2]. According to Cassie’s equation, the contact angle  $\theta$  of a heterogeneous surface consisting of two materials is given by

$$\cos \theta = \alpha_1 \cos \theta_1 + \alpha_2 \cos \theta_2 \quad (1)$$

where  $\theta_i$  is the contact angle on a homogeneous surface of pure material  $i$  and  $\alpha_i$  is the fractional area of material  $i$ . In our LBM simulations, the attraction force between a solid ( $\mathbf{x}_s$ ) and a fluid ( $\mathbf{x}_f$ ) site was expressed as

$$\mathbf{F}_s = \begin{cases} K_w \rho(\mathbf{x}_f)(\mathbf{x}_s - \mathbf{x}_f), & |\mathbf{x}_s - \mathbf{x}_f| = c \\ 0, & |\mathbf{x}_s - \mathbf{x}_f| \neq c \end{cases} \quad (2)$$

The coefficient  $K_w$  is positive for attraction forces and, by adjusting its magnitude, solid surfaces with different wettability (contact angles) can be modeled easily, from wetting to non-wetting [1]. We modeled a heterogeneous solid surface consisting of two different patches:  $K_{w1} = 0.04$  and  $K_{w2} = 0.08$ . They were arranged as  $n_1 \times K_{w1}$  followed by  $n_2 \times K_{w2}$  sites, denoted as  $(n_1:n_2)$  hereafter; such patterns were repeated to cover the entire surface. The contact angles are plotted in Fig. 1. The symbols are LBM results while the solid line is a best-fit line

---

\* Corresponding author. Tel.: +1 780 492 2791; Fax: +1 780 492 2200; E-mail: daniel.y.kwok@ualberta.ca

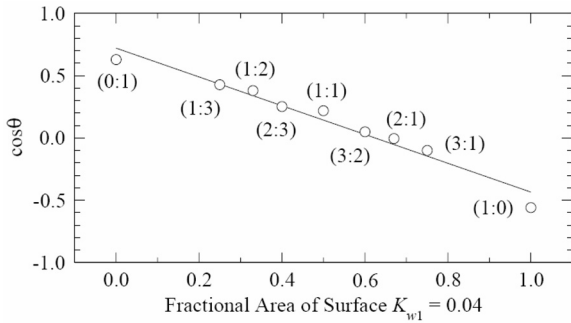


Fig. 1. Contact angles on heterogeneous surfaces with different hydrophobic ( $K_{w1} = 0.04$ ) to hydrophilic ( $K_{w2} = 0.08$ ) ratios.

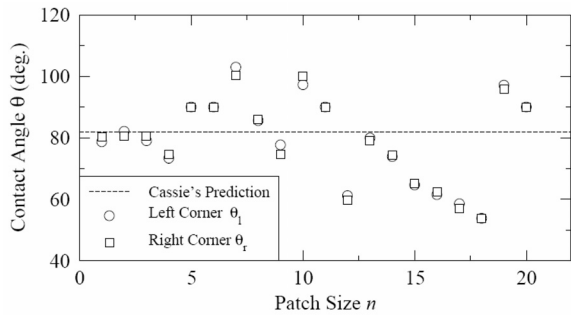


Fig. 2. Contact angles on heterogeneous surfaces consisting of 50% hydrophobic and 50% hydrophilic patches, where  $n$  represents the patch size.

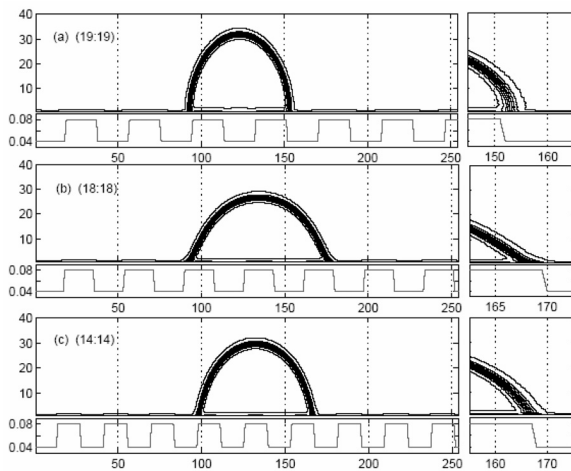


Fig. 3. Fluid density contours (upper figures) and solid attraction  $K_w$  patterns (lower figures) for three surfaces: (a) (19:19), (b) (18:18), and (c) (14:14). The figures on the right display the local features near the right contact points.

according to Eq. (1). Clearly, the results are in good agreement with Cassie's prediction; the minor deviations are within a measurement error of degrees.

The effect of patch size on contact angles was also examined. The ratio was fixed ( $\alpha_1 = \alpha_2 = 0.5$ ) and the patch size changed from (1:1) up to (20:20). The results are shown in Fig. 2 for contact angles at the left and right contact points. When the patch size is small ( $n \leq 3$ ), the angles are consistent with Cassie's prediction (81.8 degrees, dashed line in Fig. 2). For a larger patch size ( $n > 4$ ), there exist many metastable contact angle values, which deviate from Cassie's prediction. As the liquid-vapor interface has a thickness of  $\sim 6$  lattice units, it appears that the validity of the Cassie equation depends on how much the liquid-vapor interface can 'see' the patches.

To further verify the above analysis, we plotted in Fig. 3 the fluid density contours and the solid attraction strength  $K_w$  for three specific cases: (19:19), (18:18), and (14:14). The respective solid-liquid contact area ratios are  $(A_{0.04}/A_{0.08})_{(19:19)} \sim 1/2$ ,  $(A_{0.04}/A_{0.08})_{(18:18)} \sim 2/3$ , and  $(A_{0.04}/A_{0.08})_{(14:14)} \sim 2/3$ . Despite the similarity in the contact area ratios for the (18:18) and (14:14) surfaces, their contact angles are different. The contact area of surface (19:19) has a larger hydrophilic fraction, and yet its contact angle is the largest; this is due to the fact that the liquid-vapor interface sits almost completely on top of the hydrophobic patch ( $K_w = 0.04$ ). On the contrary, such an interface sits on the hydrophilic fraction ( $K_w = 0.08$ ) of the surface (18:18) and thus produces a smaller angle. For the (14:14) surface, the interface sees both of the hydrophobic and hydrophilic patches on the surface, resulting in an intermediate contact angle. Thus, the Cassie equation appears to be valid only when the patch size is on the order of the liquid-vapor interfacial thickness. These results imply, at a macroscopic scale, that the Cassie equation is, in general, not valid as it is nearly impossible to pattern a surface having regular hydrophobic and hydrophilic patches on the order of the interfacial thickness ( $\sim 1$  nm).

### 3. Apparent slip over solid-liquid interface with no-slip boundary conditions

Recent experiments [3,4] indicate significant slip on solid surfaces. Due to the difficulties in direct microscopic observation, MD [5] has been used to study the relationship between fluid slip and the properties of fluid and solid. In general, both experimental and MD simulation results show that there is a strong relationship between the magnitude of slip and the solid-fluid interaction: the weaker the interaction, the larger is the contact angle and hence the slip. Several LBM attempts have also been conducted to study this phenomenon [6-8]. However, all these attempts failed to relate the slipping magnitude with the solid-fluid interactions, which indeed plays a dominant role in such phenomenon.

Typical density and velocity profiles of pressure-driven Poiseuille flows from our simulations are displayed in Fig. 4. Here, the solid–fluid interactions were modeled as exponentially decaying attraction forces. Unlike the constant density distribution from the general LBM,

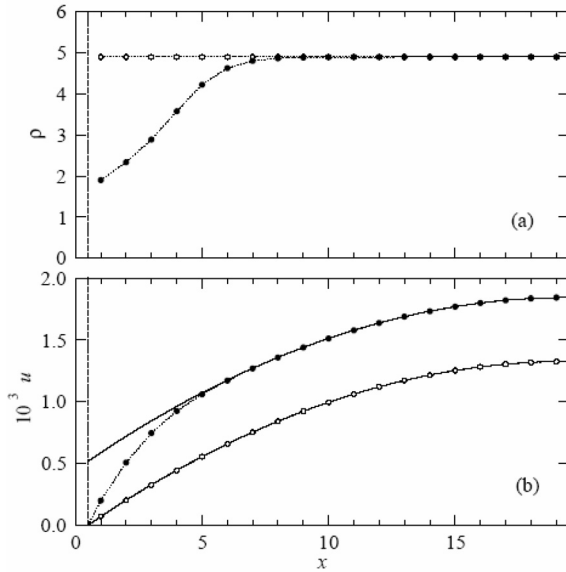


Fig. 4. (a) Density and (b) velocity profiles (half) from the mean-field LBM ( $K_w=0$ , ●) and that from a standard LBM (○). Solid lines in (b) are parabolic fittings using only the data points ( $x > 10$ ) away from the solid wall (dashed line at  $x = 0.5$ ).

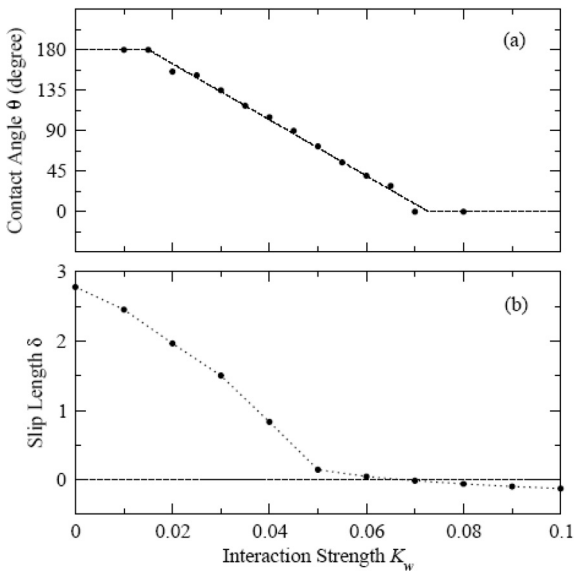


Fig. 5. Variation of (a) contact angle  $\theta$  and (b) slip length  $\delta$  with the solid–fluid interaction strength  $K_w$ .

there is a dry (low-density) layer between the bulk liquid and the wall (at  $x=0.5$ ) from our mean-field model (Fig. 4a). Comparing the two velocity profiles in Fig. 4b, we found that the no-slip BC is satisfied. Through a parabolic fitting for the data points ( $x \geq 10$ ), we found that the velocity data from a general LBM follow the curve exactly, whereas those from the mean-field LBM show good agreement only for where the density is approximately constant. Extrapolating these fitted profiles to zero velocity yields a slip length  $\delta$ . The slip lengths found in this specific example are 2.78 and 0 for the mean-field and general LBM, respectively. Overall, the velocity profile from the mean-field LBM model is qualitatively similar to those obtained from MD simulations [5].

In Fig. 5, we plotted the contact angle  $\theta$  and slip length  $\delta$  values against the solid–fluid interaction strength  $K_w$ . As solid–fluid interaction increases, the slip length decreases quickly and becomes negative when  $K_w > 0.06$ . Similar negative and small slip lengths also have been observed in MD simulations [5]. Focusing on the contact angle and slip length behaviors, we see that they follow similar decreasing trends as the solid–fluid attraction increases.

#### 4. Summary

By employing the mean-field LBM model, we have investigated several interfacial phenomena. Contact angle behaviors on heterogeneous surfaces with different patterns and patch sizes were studied. Our results suggest that Cassie’s relation is, in general, not valid in macroscopic contact angle measurements. These findings agree well with thermodynamics analysis and provide a more physical picture near the contact point. We have also studied the apparent solid–liquid interfacial slipping from a specific solid–fluid interaction. This represents the first attempt to relate the slip magnitude to the solid–fluid interactions through a LBM approach. Even with a no-slip BC applied, apparent slipping can be observed because of the specific solid–fluid interactions. Larger slip was found on more hydrophobic surfaces. With strong interactions, a small negative slip length was also observed. These results are in good agreement with those of other experimental and numerical studies. These simulations have demonstrated the potential of our mean-field free-energy LBM model in future fluid interfacial studies.

#### References

[1] Zhang J, Li B, Kwok DY. Mean-field free-energy approach to the lattice Boltzmann method for liquid–

- vapor and solid–fluid interfaces. *Phys Rev E* 2004;69:032602.
- [2] Cassie ABD. Contact angles. *Discuss Faraday Soc* 1948;3:11–16.
- [3] Trethewey DC, Meinhart CD. Apparent fluid slip at hydrophobic microchannel walls. *Physics Fluids* 2002;14:L9–L12.
- [4] Zhu Y, Granick S. Limits of the hydrodynamic no-slip boundary condition. *Phys Rev Lett* 2002;88(10): 106102.
- [5] Cieplak M, Koplik J, Banavar JR. Boundary conditions at a fluid–solid interface. *Phys Rev Lett* 2001;86:803.
- [6] Succi S. Mesoscopic modeling of slip motion at fluid–solid interfaces with heterogeneous catalysis. *Phys Rev Lett* 2002;89:064502.
- [7] Nie XB, Doolen GD, Chen SY. Lattice–Boltzmann simulations of fluid flows in MEMS. *J Stat Physics* 2002;107:279–289.
- [8] Lim CY, Shu C, Niu XD, Chew YT. Application of lattice Boltzmann method to simulate microchannel flows. *Physics Fluids* 2002;14:2299–2308.